

AD736924

NAVAL AIR DEVELOPMENT CENTER

WARMINSTER, PA. 18974

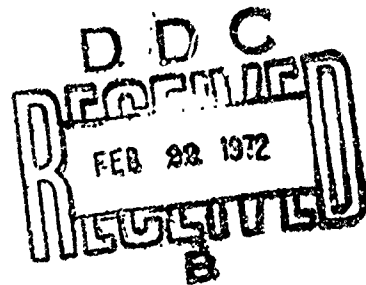
Report No. NADC-AE-7120

11 Jan 1972

HYDRODYNAMIC EFFECTS OF
HARMONIC ACCELERATION

FINAL INDEPENDENT DEVELOPMENT REPORT
TASK NO. ZR011-G1-01
Work Unit No. ES-1-01

APPROVED FOR PUBLIC RELEASE; DISTRIBUTION UNLIMITED



46

NOTICES

PRODUCT ENDORSEMENT - The discussion or instructions concerning commercial products herein do not constitute an endorsement by the Government nor do they convey or imply the license or right to use such products.

TEST		WHITE SECTION	<input checked="" type="checkbox"/>
DOC.		DIFF. SECTION	<input type="checkbox"/>
THANKED			<input type="checkbox"/>
IFICATION			
DISTRIBUTION/AVAILABILITY CODES			
OUT.	AVAIL.	NOA/IN	SPECIAL
A			

UNCLASSIFIED

DOCUMENT CONTROL DATA - R & D		
AERO-ELECTRONIC TECHNOLOGY DEPARTMENT NAVAL AIR DEVELOPMENT CENTER WARMINSTER, PENNSYLVANIA 18974		UNCLASSIFIED
HYDRODYNAMIC EFFECTS OF HARMONIC ACCELERATION		
FINAL INDEPENDENT DEVELOPMENT REPORT		
ROGER A. HOLLER		
11 JANUARY 1972	44	28
TASK NO. ZR011-01-01 WORK UNIT NO. ES-1-01	NADC-AE-7120	
	Any other report that may be associated with this report.	
APPROVED FOR PUBLIC RELEASE; DISTRIBUTION UNLIMITED		
		NAVAL AIR SYSTEMS COMMAND DEPARTMENT OF THE NAVY
<p>Circular disks, cylinders, and tandem disks are oscillated in water and the hydrodynamic mass and damping determined. Correlation with the acceleration modulus v^2/ad and nondimensional amplitude of oscillation is shown. Equations are given for coefficients of hydrodynamic inertia, drag, and total resistance for disks and methods of application to sonobuoy suspension systems are outlined.</p>		

DD FORM 1473

UNCLASSIFIED

Security: (losses) 0.10

ACCELERATION
HYDRODYNAMIC EFFECTS
DISKS
VIRTUAL MASS



DEPARTMENT OF THE NAVY
NAVAL AIR DEVELOPMENT CENTER
WARMINSTER, PA. 18974

Aero-Electronic Technology Department

REPORT NO. NADC-AE-7120

11 January 1972

HYDRODYNAMIC EFFECTS OF
HARMONIC ACCELERATION

FINAL INDEPENDENT DEVELOPMENT REPORT
TASK NO. ZR011-01-01
Work Unit No. ES-1-01

Circular disks, cylinders, and tandem disks are oscillated in water and the hydrodynamic mass and damping determined. Correlation with the acceleration modulus v^2/ad and nondimensional amplitude of oscillation is shown. Equations are given for coefficients of hydrodynamic inertia, drag, and total resistance for disks and methods of application to sonobuoy suspension systems are outlined.

Reported by:

R. Holler

R. Holler
Sonar Sensors Division

Approved by:

G. A. Gimber

G. Gimber, Superintendent
Sonar Sensors Division

D. W. Mackiernan

D. W. Mackiernan
Technical Director

APPROVED FOR PUBLIC RELEASE; DISTRIBUTION UNLIMITED

S U M M A R Y

INTRODUCTION

When a force is impressed upon a body immersed in a fluid continuum, the resultant motion of the body is determined not by the impressed force alone, as it would be in vacuo, but by the impressed force and the forces arising from the body-fluid interaction.

If the body moves linearly with constant velocity through an otherwise undisturbed homogeneous, incompressible fluid with sufficiently remote boundaries, or if there is a uniform (constant velocity) flow of the fluid past the body, the interaction force can be described as a resistance, or drag. However, the body-fluid interaction for unsteady motions is not adequately described by the drag for uniform linear motion. Corresponding relationships must be developed for the accelerating body. An attempt to describe the acceleration-induced resistance leads to the concept of virtual mass.

Motion of a body in a fluid medium results in the interdependent phenomena of boundary layer, wake, and mass transport. For steady motion, a total, or composite, drag, which includes deformation drag, friction drag, and pressure drag, is defined, expressing the resistance to motion as a quadratic law containing an empirical nondimensional drag coefficient. The total drag depends on the velocity, body geometry, and physical properties of the fluid, the parameters controlling the wake and boundary layer. Although a net fluid mass transport occurs, it does not contribute to the drag.¹ Only when acceleration takes place does the effect of transported fluid mass become a factor in resistance.

When a body is accelerated in a fluid, an inertial force occurs because a mass of fluid is also accelerated. In other words, the force which acts to impart kinetic energy to the body, through the body-fluid interaction, imparts kinetic energy to the surrounding fluid, as well.

The total mass being accelerated, or apparently being accelerated, is called the virtual mass. Therefore, the virtual mass is the sum of the physical mass of the body and the hydrodynamic mass (often termed "added" mass or "induced" mass). The hydrodynamic mass corresponds to a volume of fluid defined conventionally in simple geometrical terms. The simplified concept of an entrained fluid mass moving with the body represents a complex phenomenon of body-fluid interaction which plays an important part in hydrodynamics.

Sonobuoy systems consist of essentially three elements: a surface float, a hydrophone, and an intermediate suspension. As the surface float is required to maintain an exposed antenna, it is designed to

1. See References, page 25.

follow the ocean surface with a constant freeboard. The hydrophone, on the other hand, is susceptible to adverse dynamic effects and is required to be virtually motionless.^{2,3} The function of the intermediate suspension is to prevent the transmission of motion of one to the other.

A hydrophone suspension invariably takes the form of a simple spring-mass system or series of spring-mass systems. It is so designed that its natural frequency is below the range of ocean wave frequencies, and therefore, the motion amplitude of the hydrophone is attenuated from that of the surface float. The smaller the natural frequency of the suspension, the more effective the suspension is.

Three parameters affect the natural frequency - mass, spring constant, and damping coefficient. For a low natural frequency, mass and damping coefficient should be large, and spring constant small. The juggling of these parameters for optimum efficiency of motion isolation is influenced to a certain extent by size, weight, and packaging considerations.

Large physical mass means a heavy sonobuoy, but beyond this, a weighty lower unit limits the use of a highly elastic compliance in the suspension. To overcome this limitation on the compliance, buoyancy can be utilized to reduce weight while retaining mass. The use of buoyancy, however, vastly increases size, possibly, beyond packageability. One means of acquiring mass without significant weight or size problems is the utilization of hydrodynamic mass.

Practical utilization of hydrodynamic mass for the design of a sonobuoy suspension cannot be implemented until the phenomenon itself has been sufficiently understood and described for design criteria to be determined. These criteria have not heretofore been available. The task of ascertaining these criteria was undertaken at NAVAIRDEVCON under Independent Research Task No. ZR011-01-01, Work Unit No. ES-1-01.

RESULTS AND CONCLUSIONS

1. The hydrodynamic mass and acceleration resistance effects of oscillating disks, cylinders, and tandem disks have been determined through measurement of the frequency and amplitude of motion at resonance of a spring-mass system.
2. The hydrodynamic effects on oscillating disks (and other bodies) can be expressed in terms of coefficients of hydrodynamic inertia, drag, and total resistance, and can be correlated by the acceleration modulus v^2/ad , which is a measure of motion amplitude, although no correlation with Reynolds number is apparent.

^{2,3} See References, page 25.

3. The hydrodynamic coefficients describing a disk in harmonic acceleration can be written as:

$$C_I = m_h/\rho d^3 = 1.2 (v^2/ad)^{1/2}$$

$$C_D = F_D/(\rho A v^2/2) = 2.2 (v^2/ad)^{-1/2}$$

$$C_T = F_T/(\rho A v^2/2) = 5.2 (v^2/ad)^{-1/2}$$

within limits of motion approximated by $0.08 \leq v^2/ad \leq 3$.

4. The hydrodynamic inertial effect is associated with the vortex formation in the wake of the accelerated body, and an anomaly occurs when the vortex is shed, causing unstable motion of the oscillating body.

5. Variation of hydrodynamic inertial effects of oscillating cylinders with length-to-diameter ratio and of oscillating tandem disks with separation-to-diameter ratio has been determined.

6. The data resulting from this investigation can be applied directly to sonobuoy suspension systems, facilitating the analysis and design of these systems.

TABLE OF CONTENTS

	P a g e
SUMMARY	iii
Introduction	iii
Results and Conclusions.	iv
LIST OF FIGURES	vii
NOMENCLATURE.	viii
BACKGROUND.	1
DISCUSSION.	3
Determination of Hydrodynamic Mass	3
Hydrodynamic Mass and Damping of Oscillating Disks	4
Cylinders and Tandem Disks	18
REFERENCES.	25
APPENDIXES	
A Determination of the Hydrodynamic Mass and Damping Constant of Oscillating Bodies.	A-1
B Application of the Data to Sonobuoy Suspensions . . .	B-1

LIST OF FIGURES

Figure	Title	Page
1	Experimental Apparatus	3
2	Drag Coefficient Versus Reynolds Number for Disks and Thin Plates in Steady Flow.	7
3	Hydrodynamic Inertia Coefficient Versus Reynolds Number for Circular Disks in Harmonic Acceleration. . .	7
4	Drag Coefficient Versus Reynolds Number for Circular Disks in Harmonic Acceleration.	8
5	Total Resistance Coefficient Versus Reynolds Number for Circular Disks in Harmonic Oscillation.	8
6	Hydrodynamic Inertia Coefficient Versus Acceleration Modulus for Oscillating Disks	11
7	Comparison of Data for Oscillating Disks and Disks in Linear Acceleration.	11
8	Damping Constant Versus Acceleration Modulus for Oscillating Disks	12
9	Drag Coefficient Versus Acceleration Modulus for Oscillating Disks	13
10	Total Resistance Coefficient Versus Acceleration Modulus for Oscillating Disks	13
11	Comparison of Total Resistance Coefficient Data of Disks in Harmonic and Linear Acceleration.	14
12	Hydrodynamic Inertia Coefficient Versus Acceleration Modulus for 2 Long Thin Plate in Oscillatory Flow.	16
13	Hydrodynamic Inertia Coefficient Versus Length-to- Diameter Ratio for Oscillating Cylinders.	19
14	Drag Coefficient Versus Length-to-Diameter Ratio for Oscillating Cylinders	20
15	Total Resistance Coefficient Versus Length-to- Diameter Ratio for Oscillating Cylinders.	20
16	Hydrodynamic Inertia Coefficient Versus Separation- to-Diameter Ratio for Oscillating Tandem Disks.	22
17	Drag Coefficient Versus Separation-to-Diameter Ratio for Oscillating Tandem Disks.	23
18	Total Resistance Coefficient Versus Separation-to- Diameter Ratio for Oscillating Tandem Disks	24

N O M E N C L A T U R E

A	= Projected surface area normal to motion
a	= Acceleration
B	= Volume characteristic of a body
C_D	= Drag coefficient
C_I	= Hydrodynamic inertia coefficient
C_T	= Total resistance coefficient
c	= Damping constant
c_c	= Critical damping constant
d	= Diameter of body
f	= Frequency
F_D	= Drag force
F_I	= Hydrodynamic inertia force
F_T	= Total resistance force
g	= Gravitational acceleration
k	= Spring constant
ℓ	= Cylinder length
M	= Magnification, y/y_0
m	= Virtual mass, $m_h + m_p$
m_h	= Hydrodynamic mass
m_p	= Physical mass
N_F	= Froude number
N_{Re}	= Reynolds number
S_t	= Strouhal number

N O M E N C L A T U R E (c o n t i n u e d)

- s = Separation distance between tandem disks
- T_0 = Oscillation period
- T_s = Vortex shedding period
- t = Time
- v = Velocity
- x = Linear distance
- y = Amplitude of oscillatory motion
- y_0 = Input amplitude to spring-mass system
- ν = Kinematic viscosity
- ρ = Fluid density
- ω = Angular frequency, $2\pi f$
- ω_n^* = Undamped natural frequency of spring-mass system in air
- ω_{nd} = Damped natural frequency of spring-mass system in fluid

BACKGROUND

The effect of acceleration on a body in a fluid was first noted in the 1776 work of DuBuat with spherical pendulum bobs in water; then, in the early nineteenth century, Bessel, Green, and Stokes laid the theoretical foundation for the concept of virtual mass. Extensive bibliographies on early work in this subject have been presented by Torobin and Gauvin⁴ and Stelson.⁵

The theoretical basis for hydrodynamic mass arises out of potential flow considerations of the kinetic energy imparted by a moving body to an ideal, incompressible fluid of infinite extent. Milne-Thomson⁶ considered the disk as a special case of the planetary ellipsoid. From the complex potential, the kinetic energy was determined to be $\rho d^3 v^2 / 6$, for a circular disk of diameter, d , moving perpendicularly to its plane with velocity, v , in a fluid of density, ρ . The hydrodynamic mass, therefore, is

$$m_h = \rho d^3 / 3 \quad (1)$$

Kanwal⁷ considered oscillating axially-symmetric bodies at small Reynolds numbers to determine virtual mass arising in Stokes flow. The formula derived for a circular disk moving broadside to the stream for small Reynolds numbers exhibited a dependency on the square root of oscillation period. A similar result was obtained for the sphere, agreeing with the parameter presented by Carstens⁸ to describe spherical particle motion in a fluid.

The treatment of an oscillating disk by the integration of pressures method based on a vibrating circular piston in an infinite baffle⁹ results in a series solution for hydrodynamic mass. At high frequencies, the value of hydrodynamic mass is approximated to exhibit a dependence on the square of oscillation period, and at lower frequencies, m_h approaches $\rho d^3 / 3$, the same value obtained in equation (1). The assumption of this method is that the amplitude of oscillation be extremely small, since no account is taken of boundary layer formation.

The conditions of an incompressible, irrotational ideal fluid under which the results of potential flow theory apply are difficult to achieve with real fluids in any but very limited situations. For a circular disk in flowing water, Stanton and Marshall¹⁰ found a vortex-ring to have formed at a Reynolds number of 5, and vortex shedding to have begun at $N_{Re} = 195$. Simmons and Dewey,¹¹ Willmarth, et al,¹² and others have reported the critical Reynolds number for vortex-related instability-onset in disk motion as 100. Once vortex formation occurs, the theoretical solutions have no great practical importance.

5-12 See References, page 25.

Small amplitude oscillations do approximate the conditions of the theory, and the way in which the hydrodynamic mass behaves in this area is of interest. Stelson⁵ reported on experiments with bodies oscillating in fluid with amplitudes on the order of 0.01 inch at frequencies between 14 and 35 Hz. For 2-inch diameter disks, the values of hydrodynamic mass obtained were in good agreement with the theoretical value, being slightly larger when disk thickness was increased. Similarly small amplitudes (0.002 to 0.011 diameter) for disks vibrating in water at 10.31 Hz were employed by Bramig¹³ who reported values of hydrodynamic mass below the theoretical value but approaching it as the amplitude decreased. Carstens⁶ noted the effect of increasing amplitude of oscillation on submerged spheres to be a reduction of hydrodynamic mass from the theoretical value.

The indication, in the works of both Bramig and Carstens, that hydrodynamic mass decreases as the amplitude of oscillation increases, is misleading, because larger amplitude oscillation experiments performed more recently denote the opposite trend. This apparent contradiction probably occurs because of the different flow regimes in which the experiments took place.

The conditions of turbulent flow, which accompany any appreciable motion of a bluff body in a real fluid, have been encountered in experiments involving both linear motion and oscillation. Significant results have been obtained for linear motion by Iversen and Balent¹⁴ and Luneau¹⁵ for disks, Keim¹⁶ for cylinders, and Bugliarello¹⁷ and Lunnon¹⁸ for spheres. Oscillatory motion has been investigated for cylinders and flat plates by Keulegan and Carpenter¹⁹ and McNown and Keulegan,²⁰ for cylinders and spheres by Crooke,²¹ and for various bodies by Patton.²² Many of these investigations have been summarized by Torobin and Gauvin⁴ and by Wiegel.²³ The hydrodynamic mass determined in these investigations for several bluff bodies in two distinct modes of accelerated motion was larger than the theoretical value for potential flow and showed a distinct anomaly when vortex shedding was initiated. Further reference to these investigations is made in the subsequent discussion of the results of the present study.

13-23 See References, pages 25 and 26.

DISCUSSION

DETERMINATION OF HYDRODYNAMIC MASS

The experimental technique used to measure the hydrodynamic mass of bodies in high amplitude oscillation was the natural frequency method. This consisted of measuring the shift in resonant frequency and the amplification of body excursion for the spring-supported body in water and air. In this manner, the effect of fluid damping was determined at the same time as hydrodynamic mass.

Apparatus

The experiments were undertaken using 1/16-inch thick aluminum disks of 2, 4, 6, and 12-inch diameters, and a 12-inch diameter fiberglass disks of the same thickness. The disk was mounted orthogonally on the end of a 1/4-inch diameter rigid rod, attached at its center, and the rod was suspended from a helical spring. A variable speed drive, with adjustable input (forcing) amplitude from 1.5 to 5.5 inches, was used to oscillate the top end of the spring through a range of frequencies. The experimental setup is illustrated in figure 1.

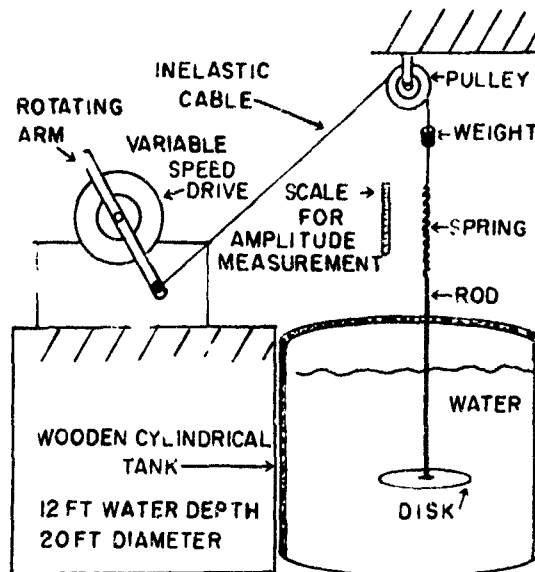


FIGURE 1 - Experimental Apparatus

The springs were fabricated of piano wire wound in close coils. The helical springs were designed to have negligible damping. With appropriate masses, the springs exhibited internal damping ratios $c/c_c < 0.005$. The springs were determined to be linear and the spring constants were invariable.

The water tank was cylindrical, having a depth of 16 feet and a diameter of 20 feet. The disks were submerged in tap water to a mean depth of 4 feet. Experiments were spheres by Stelson⁵ indicated 2 diameter submergence produced negligible free surface effects. Murtha²⁴ places this depth limit at 2.5 diameters for cylinders; Patton,²² at 5 diameters for spheres; and Waugh and Ellis,²⁵ at 2.5 diameters for spheres. Of these investigators, only Patton experienced high amplitude oscillation. Sufficient submergence depth was considered to have been obtained for the present experiments so long as the surface was not disturbed by the disk

22-25 See References, page 26.

motion. When the disk was too close to the water surface, a definite rippling accompanied each motion cycle, and the resonant peak shifted to a higher frequency than that observed when the disk was at sufficient depth. Good agreement was obtained between the data from disks in this large tank and those from similar preliminary tests in a 2- by 2-foot square tank, having a depth of 3.5 feet, with disks up to 6-inch diameter.

Additional tests were conducted using cylinders of 2.5-inch diameter and length-to-diameter ratios of one and two. These were oscillated axially. Two similar disks in tandem were also employed.

Procedure

The spring-mass system was assumed to be adequately described by the linear single-degree-of-freedom equation:

$$m\ddot{y} + c\dot{y} + ky = F_0 \cos \omega t, \quad (2)$$

where m the virtual mass (the sum of physical mass m_p and hydrodynamic mass m_h) and c the damping coefficient for the disk in water are dependent upon the system parameters. The peak amplitude and the frequency at which it occurred were determined experimentally. This resonant frequency was considered the damped natural frequency for the system in water ω_{nd} and comparison with the undamped natural frequency in air ω_n yield equations for the hydrodynamic mass:

$$m_h = m_p \{ [(2 + Q)/6] [\omega_n/\omega_{nd}]^2 - 1 \}, \quad (3)$$

and coefficient of damping:

$$c = (m_p \omega_n^* / \omega_{nd}) \sqrt{(4 - Q)(2 + Q)/9}, \quad (4)$$

where Q (equation (A-14); appendix A) depends solely upon the magnification factor of the motion amplitude. Derivation of equations (3) and (4) are shown in appendix A.

HYDRODYNAMIC MASS AND DAMPING OF OSCILLATING DISKS

The drag of a bluff body in uniform flow is:

$$F_D = C_D \rho A v^2 / 2, \quad (5)$$

where C_D is the nondimensional drag coefficient, ρ is the fluid density, A is the projected surface area of the body normal to the direction of flow, and v is the velocity of the body relative to the fluid. For a body of a given shape, the drag is described by equation (5) and a plot of C_D versus Reynolds number, as determined by experiment.

Resistance to acceleration may be considered as a hydrodynamic inertial force:

$$F_I = m_h a = C_I \rho B a, \quad (6)$$

where B is a volume characteristic of the body, a is the body acceleration, and C_I , like C_D , may be expected to be dependent upon the condition of body motion.

Because most investigations of hydrodynamic acceleration effects consider linear motion where the inertial and drag forces act in concert, a variation of the resistance force equations has arisen:

$$F_T = C_D \rho A v^2 / 2 + C_I \rho B a = C_T \rho A v^2 / 2, \quad (7)$$

where F_T is a total resistance force, and C_T is a total resistance coefficient. In oscillatory motion where velocity and acceleration have a $\pi/2$ phase difference, the concept of a simple summation of drag and hydrodynamic inertia as if they were a single drag force would seem of dubious merit, considering the time-sequence of harmonic motion. However, the values of hydrodynamic inertia and drag obtained in this investigation resulted from evaluation of the motion cycle of the oscillating body and may be said to represent steady-state equivalents rather than instantaneous values. As both the drag and inertial forces are acting in opposition to the body motion throughout the oscillation cycle, they can, in a sense, be summed into the single resistance force in equation (7). Values for C_T have been calculated for the oscillating disk in this investigation for comparison with linear motion data reported in the literature; however, this procedure must be accompanied by appropriate notation of the phase discrepancy involved in placing the oscillatory data on the same basis as the linear data.

Because the linear single-degree-of-freedom equation was used for the calculation of hydrodynamic mass m_h and damping coefficient c , a drag coefficient corresponding to the turbulent damping was determined by equating the damping force cv to a drag force:

$$cv = C_D \rho A v^2 / 2, \quad (8)$$

defining the drag coefficient as:

$$C_D = 2c / \rho A v. \quad (9)$$

This value was employed in equation (7) for the calculation of C_T .

According to the theory of potential flow, the hydrodynamic mass is the mass of a volume of fluid equivalent to 63.7 percent of the volume of a sphere with the same diameter as the disk. This can be expressed more simply as $\rho d^3/3$. Therefore, the volume B in equation (6) is chosen as d^3

rather than the volume of a sphere, as the spherical volume has no particular physical significance for the disk. The inertia coefficient C_I for potential flow is simply one-third, and in general:

$$C_I = m_h / \rho d^3 \quad (10)$$

Correlating Modulus

Dimensional analysis yields a number of nondimensional groups descriptive of the body-fluid interaction. Those groups that are possibly meaningful to this investigation include:

1. Reynolds number, $N_{Re} = vd/\nu$;
2. Froude number, $N_F = v/\sqrt{gd}$;
3. Acceleration modulus, ad/v^2 ;
4. Acceleration rate of change modulus, $\dot{a}d^2/v^3$; and
5. Time modulus, vt/d .

One or several of these dimensionless groups may be useful in correlating the data in the form of the nondimensional coefficients C_I , C_D , and C_T .

Free surface effects were found to be negligible in this investigation, as the test body was submerged to sufficient depth. Therefore, the Froude number was not an influence upon the resistance to acceleration.

Reynolds number reflects the influence of viscous forces and is important in the correlation of drag coefficients for uniform flow. The drag coefficients for disks and thin plates in constant velocity motion are shown in figure 2. Using the maximum harmonic velocity for calculation of the Reynolds number, the values of C_I , C_D , and C_T for the oscillating disk are plotted in figures 3, 4, and 5 against Reynolds number. No distinct correlation occurs. This agrees with the results of most investigators.

Torobin and Gauvin,⁴ in summarizing the literature of accelerated motion effects, noted a trend for the effect of acceleration on drag coefficient to be reduced as the Reynolds number, and therefore, the turbulent component of the wake structure, was increased. There is not sufficient evidence in the data of this investigation to substantiate that reported trend.

The acceleration modulus, first employed by Iversen and Balent,¹⁴ has proved valuable in correlating the data of acceleration-induced resistance. The modulus ad/v^2 has a significance that has been overlooked or ignored by investigators in this area. To discuss this point, it is convenient to define the reciprocal acceleration modulus v^2/ad .

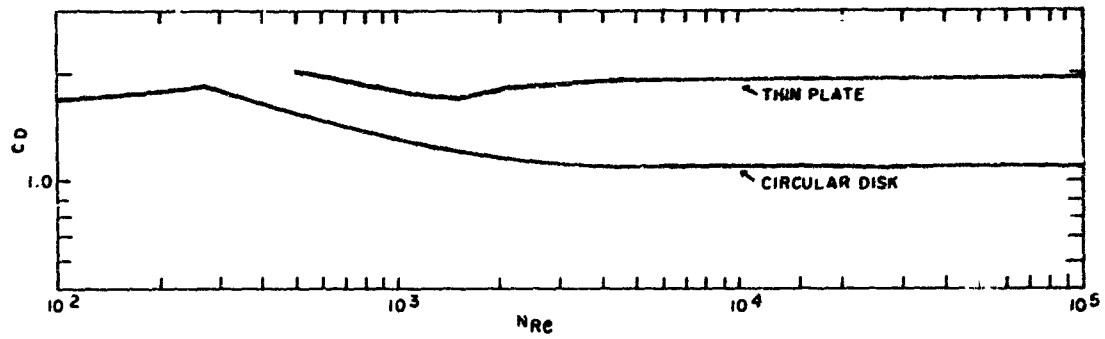


FIGURE 2 - Drag Coefficient Versus Reynolds Number for Disks and Thin Plates in Steady Flow

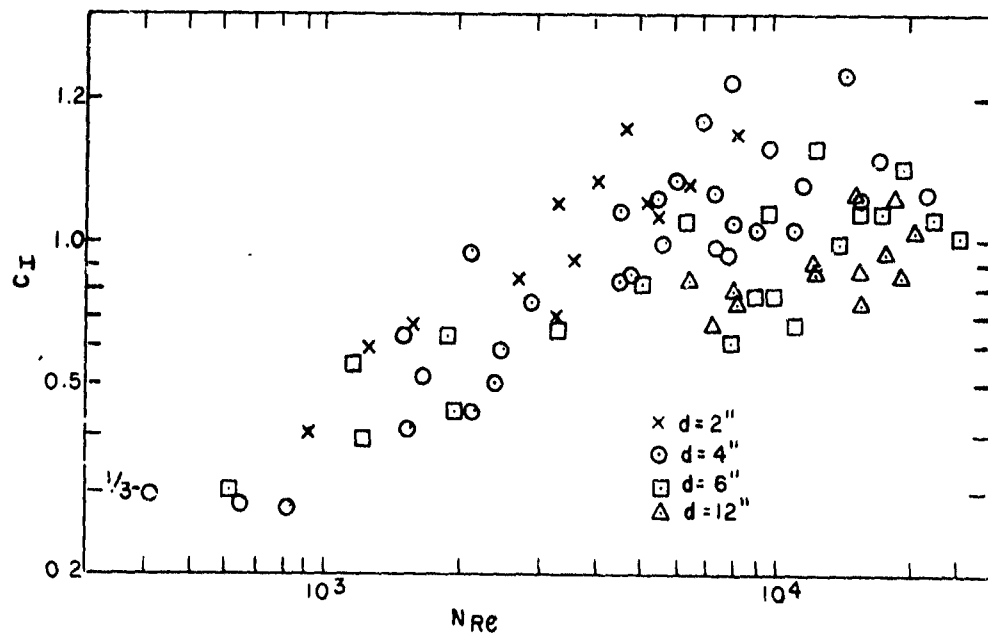


FIGURE 3 - Hydrodynamic Inertia Coefficient Versus Reynolds Number for Circular Disks in Harmonic Acceleration

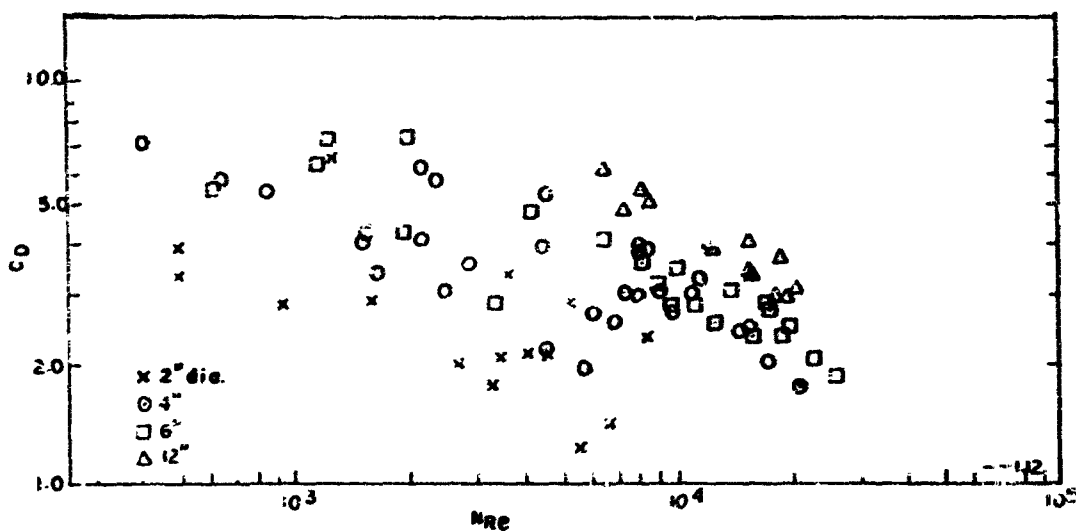


FIGURE 4 - Drag Coefficient Versus Reynolds Number for Circular Disks in Harmonic Acceleration

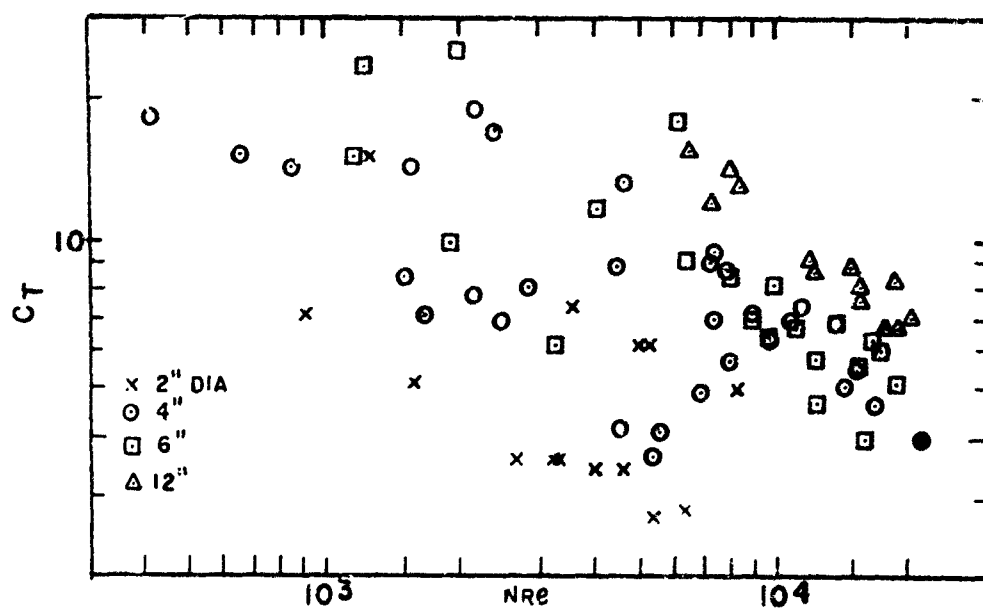


FIGURE 5 - Total Resistance Coefficient Versus Reynolds Number for Circular Disks in Harmonic Oscillation

Considering the motion of a body accelerated from rest at a constant acceleration, then:

$$\begin{aligned} a &= \ddot{x} = \text{const} \\ v &= \dot{x} = at \\ x &= x = at^2/2. \end{aligned} \quad (11)$$

The modulus reduces to a measure of the distance travelled:

$$v^2/ad = 2x/d. \quad (12)$$

It can be shown that similar results, with differences in proportionality constants, can be obtained for linear motion associated with practically any continuously acting monotonic acceleration.

In the case of oscillatory motion, maximum values are:

$$\begin{aligned} a &= \ddot{y} = y\omega^2; \\ v &= \dot{y} = y\omega; \\ y &= y; \end{aligned} \quad (13)$$

and the acceleration modulus reduces to:

$$v^2/ad = y/d. \quad (14)$$

This result imparts a physical significance to the v^2/ad modulus and indicates the relationship between linear and oscillatory motions.

The rate of change of acceleration modulus for oscillation is simply:

$$v^3/\dot{a}d^2 = (y/d)^2, \quad (15)$$

and can be considered within the framework of the modulus v^2/ad .

The time modulus vt/d has been used by Keulegan and Carpenter¹⁹ with success in correlating the data of plates and cylinders in oscillating flow. For oscillation, it is apparent that time modulus and acceleration modulus are closely related:

$$vt/d = v/fd = y\omega/fd = 2\pi y/d. \quad (16)$$

As it would be superfluous to employ both the time modulus and the acceleration modulus to describe the motion, the succeeding discussion considers only the v^2/ad modulus.

Inertial, Drag, and Resistance Coefficients

The hydrodynamic inertia coefficient C_I for oscillating disks is shown in figure 6 as a function of the modulus v^2/ad . Correlation of the sort that could not be obtained for Reynolds number does occur for the acceleration modulus. Using the method of least squares, an approximate equation for the inertia coefficient was determined:

$$C_I = 1.2(v^2/ad)^{1/2} \quad (17)$$

for $0.08 < v^2/ad < 3$. For values of $v^2/ad < 0.08$, the coefficient $C_I = 1/3$, the theoretical value. When $v^2/ad > 3$, the disk motion became erratic and measurements could not be made.

Iversen and Balent¹⁴ and Luneau¹⁵ investigated the acceleration effects on circular disks in linear motion. The former operated with variable acceleration (decreasing with time) and the latter with constant acceleration. Their results are compared with those of the present investigation in figure 7. It should be noted that the three curves represent different relationships between v^2/ad and y/d . For example, Luneau's v^2/ad modulus is twice the distance travelled divided by disk diameter [equation (12)], and the v^2/ad modulus for the present investigation is one-half the total excursion of the oscillating disk divided by the diameter [equation (14)]. If these two curves were plotted on a scale of equivalent distance travelled in diameters, they would fall much closer together.

When the damping constant c of equation (2) is plotted against v^2/ad , no correlation occurs (figure 8). However, when the damping constant is converted into a drag coefficient by equation (9), correlation with v^2/ad results, as shown in figure 9.

Employing equation (7), a total resistance coefficient C_T was plotted in figure 10. A least squares computation lead to the approximation:

$$C_T = 5.2(v^2/ad)^{-1/2}. \quad (18)$$

From equations (7), (17), and (18):

$$C_D = 2.2(v^2/ad)^{-1/2}. \quad (19)$$

A comparison of the data of the present investigation for oscillating disks with the linear motion data for disks from Iversen and Balent and Luneau is shown in figure 11. The conditions of potential theory for hydrodynamic mass and of steady flow drag are shown as limiting values after the technique of Burgliarello,¹⁷ whose data on spheres followed similar trends.

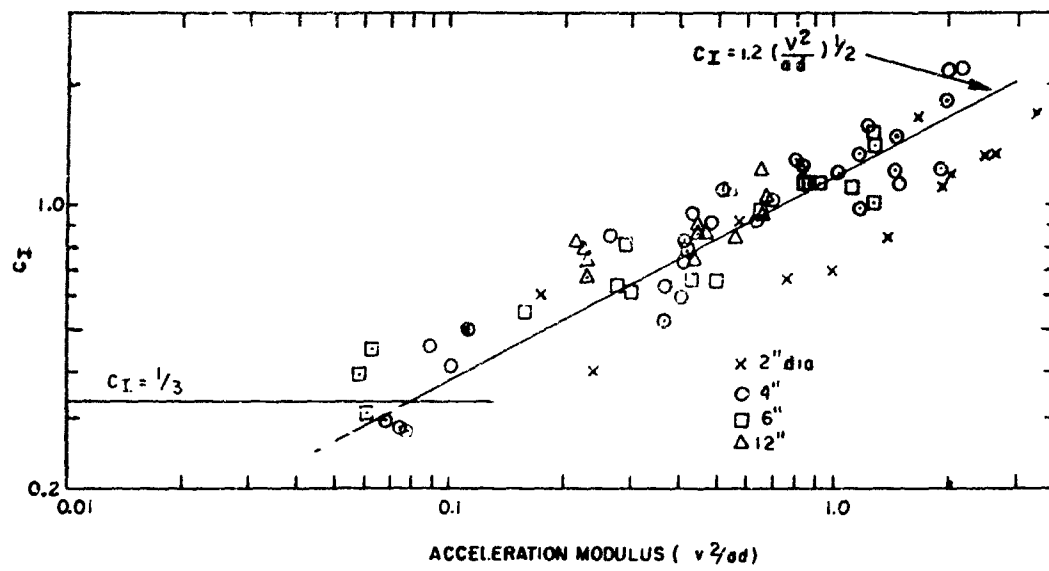


FIGURE 6 - Hydrodynamic Inertia Coefficient Versus Acceleration Modulus for Oscillating Disks

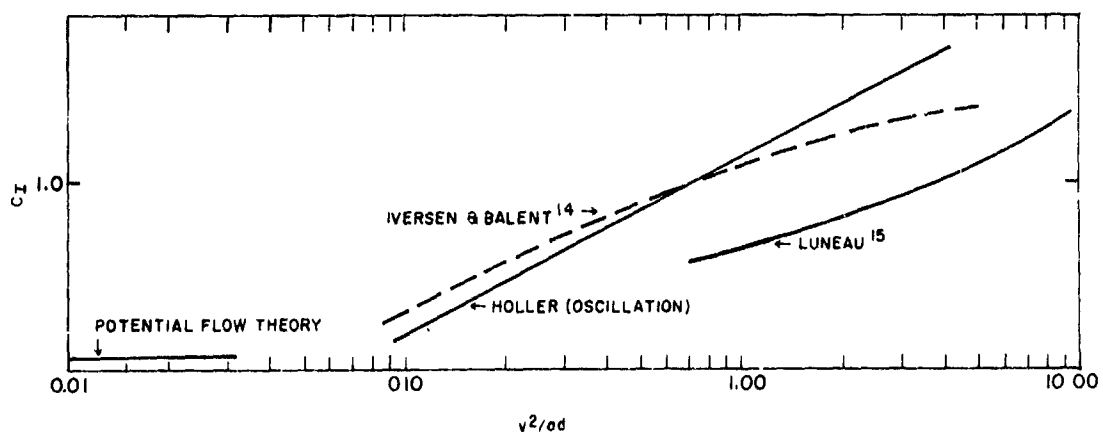


FIGURE 7 - Comparison of Data for Oscillating Disks and Disks in Linear Acceleration

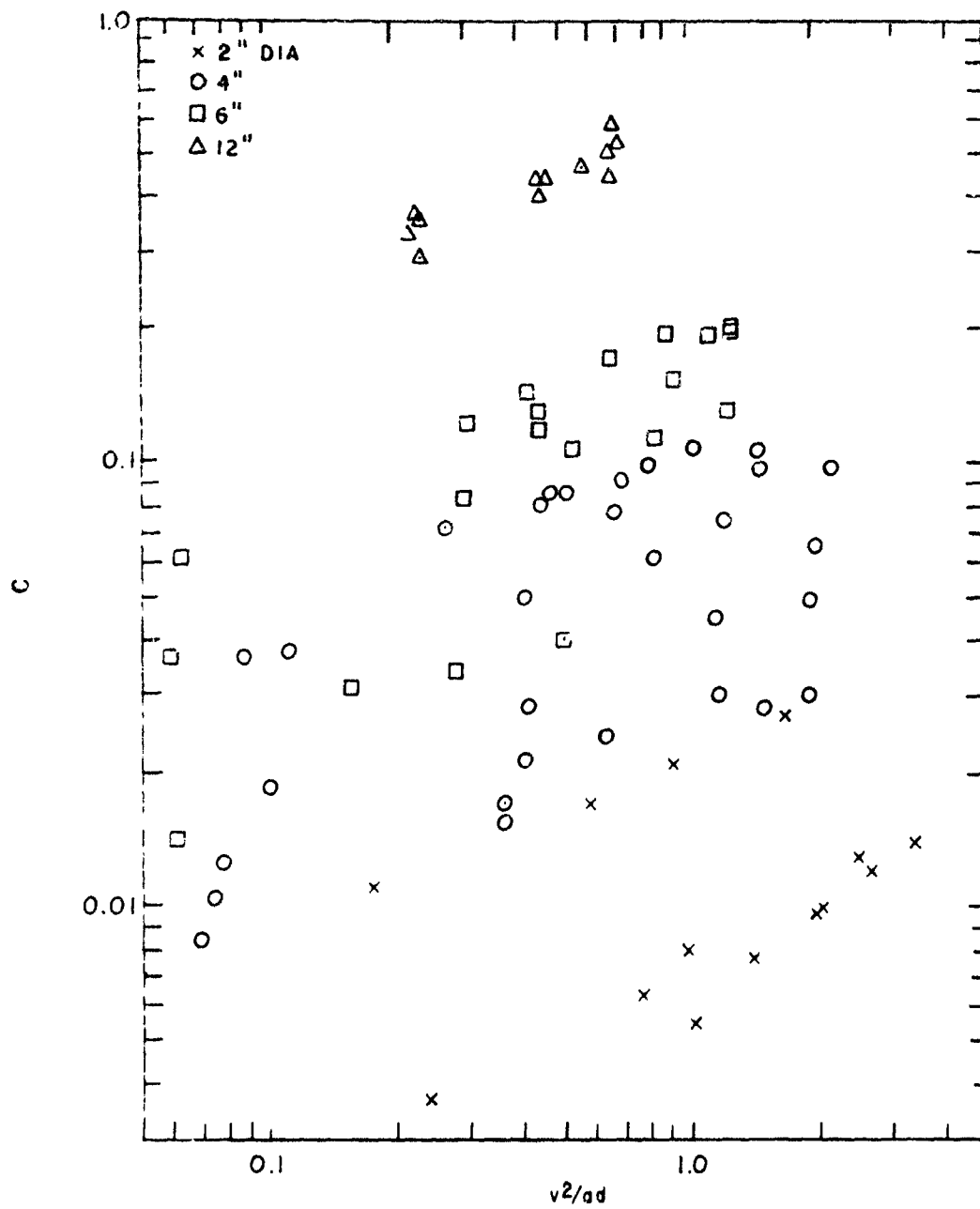


FIGURE 8 - Damping Constant Versus Acceleration Modulus for Oscillating Disk.

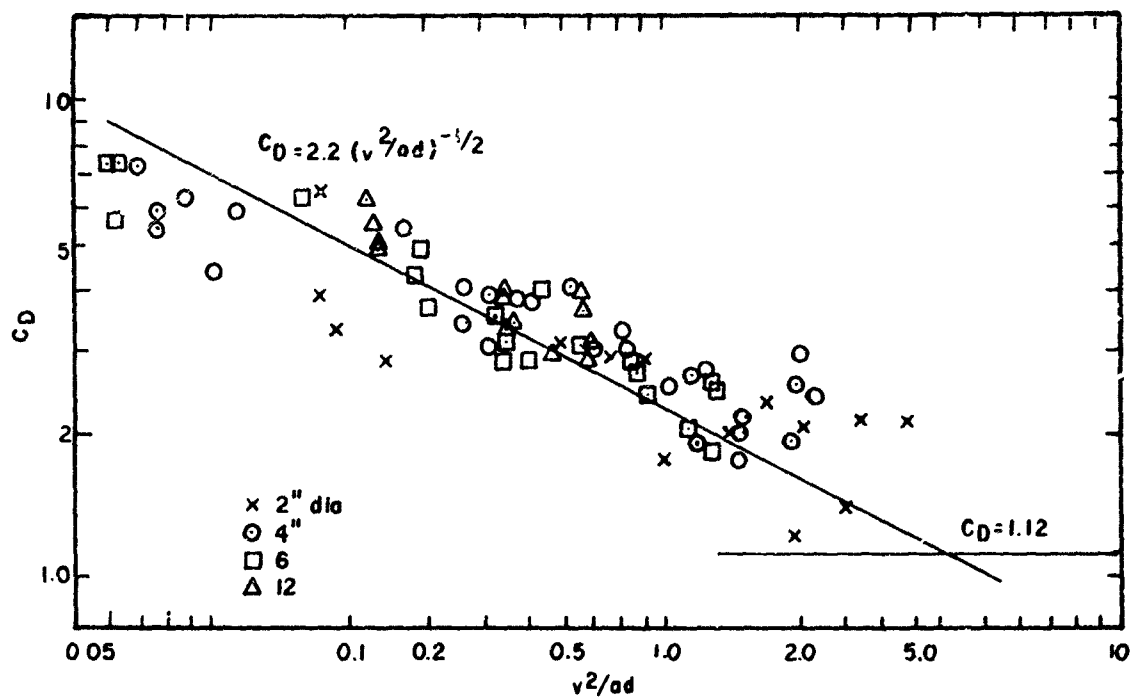


FIGURE 9 - Drag Coefficient Versus Acceleration Modulus for Oscillating Disks

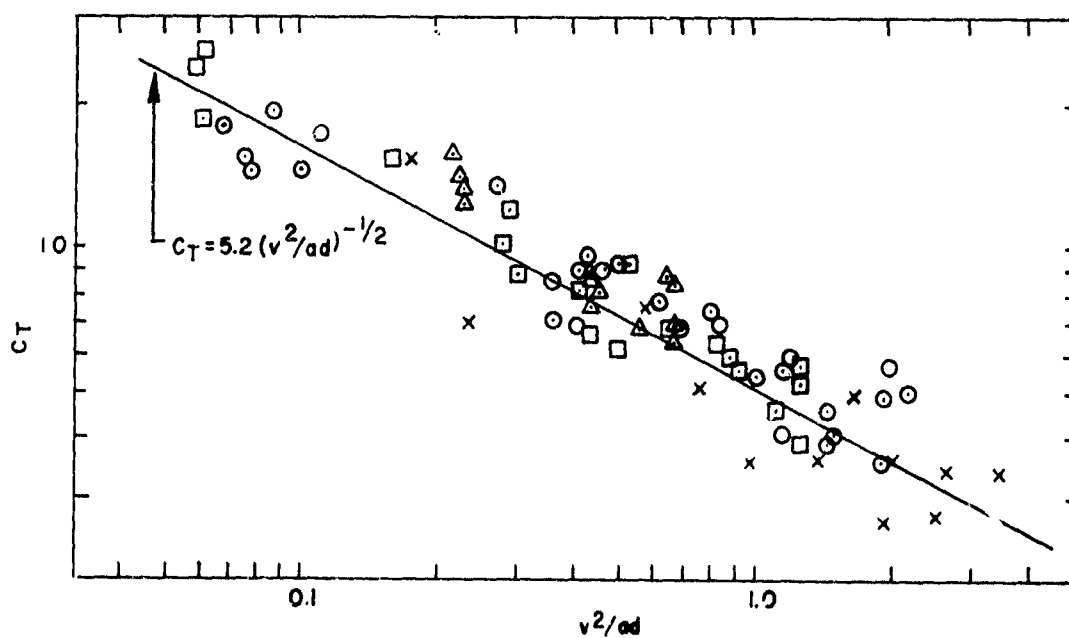


FIGURE 10 - Total Resistance Coefficient Versus Acceleration Modulus for Oscillating Disks

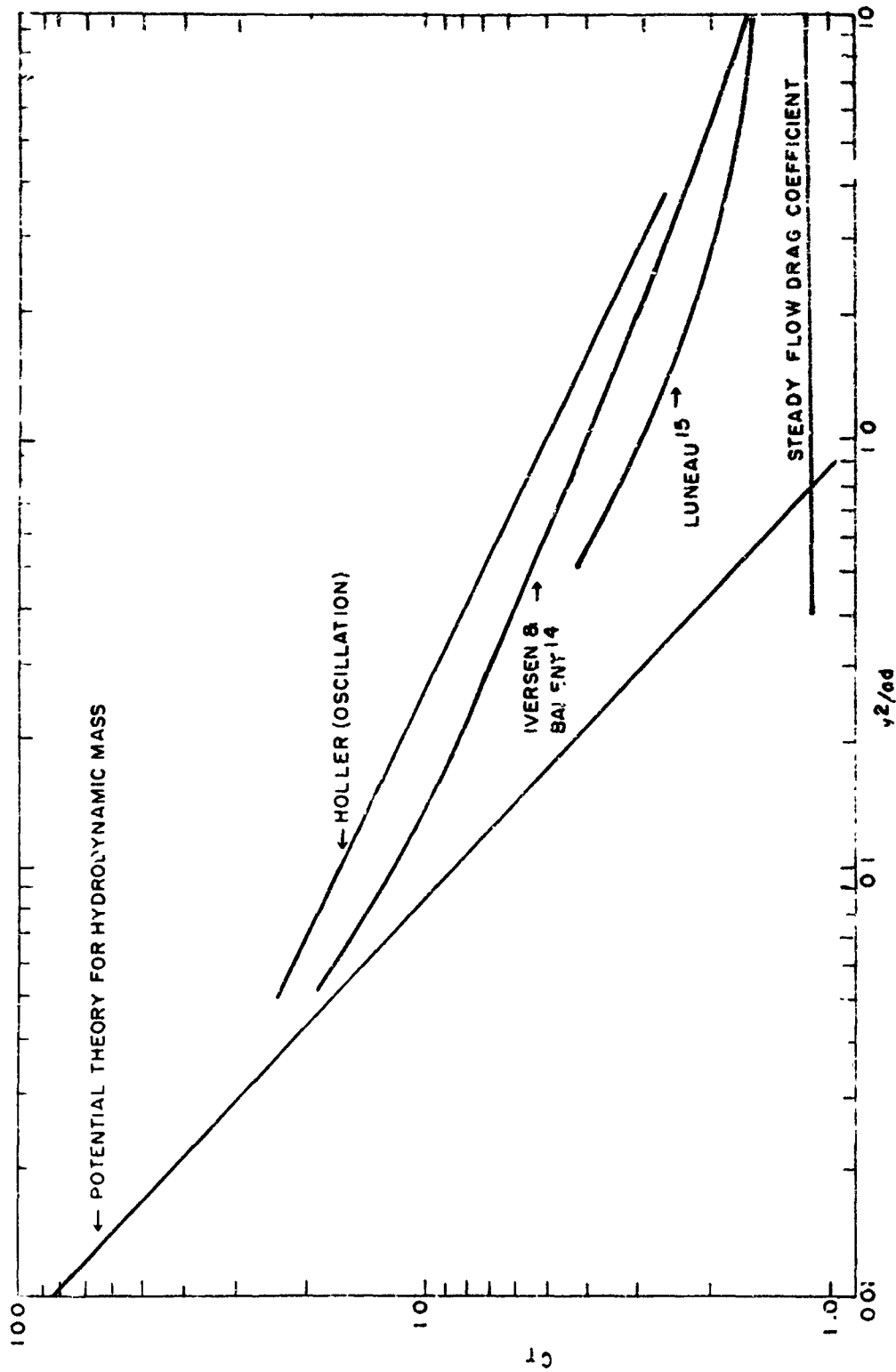


FIGURE 11 - Comparison of Total Resistance Coefficient Data of Disks in Harmonic and Linear Acceleration

Disks of square, hexagonal, and octagonal shape, having the same area as the circular disk, were employed in a limited number of experiments and yielded results that differed imperceptibly from those obtained with circular disks.

Vortex Formation

When a bluff body moves linearly through a fluid with a constant velocity, vortex formation and shedding occurs in the wake with a period defined by:

$$T_s = d/S_t v, \quad (20)$$

where S_t is a Strouhal number (nearly constant over a wide Reynolds number range). Bodies moving with different constant velocities shed vortices at different periods; however, for steady flow conditions $v = x/t$, the displacement x of the body during each shedding cycle is the same, independent of the velocity:

$$x = d/S_t. \quad (21)$$

For a flat plate normal to the flow, the Strouhal number was reported by Lehnert²⁶ to be 0.147 for Reynolds numbers above 4000. Since the vortex shedding from a plate occurs in alternate fashion, first from one side then from the other, the distance of travel for the shedding of a vortex pair is 6.8 diameters. Therefore, there is a 3.4 diameter spacing between shed vortices.

If the flat plate were oscillated normal to its surface, the amplitude of oscillation y would be just half the total excursion in one direction. To obtain a condition such that no vortices were shed during the cycle except at the points of direction reversal, the amplitude of oscillation must be limited to $y = 1.7 d$.

Keulegan and Carpenter¹⁹ employed a stationary flat plate in oscillating flow to measure the hydrodynamic mass coefficient in a range of Reynolds numbers, based on maximum velocity, between 5,000 and 15,000. The data were correlated by the time modulus vt/d using the maximum velocity $v = 2\pi y/T_0$, where T_0 is the oscillation period. Since the time modulus can be written in terms of v^2/ad [equation (14) and (16)], the data of Keulegan and Carpenter are shown in figure 12.

The value of C_m , a hydrodynamic mass coefficient related to the volume of a cylinder of fluid with the plate as its largest cross section, increases with distance travelled ($y/d = v^2/ad$) until the vortex shedding cycle coincides with the oscillation cycle. The hydrodynamic inertia begins to decrease beyond this point as vortex shedding occurs during the oscillation cycle. When the amplitude of oscillation is large enough that numerous vortices are shed per cycle, a quasi-steady condition is reached.

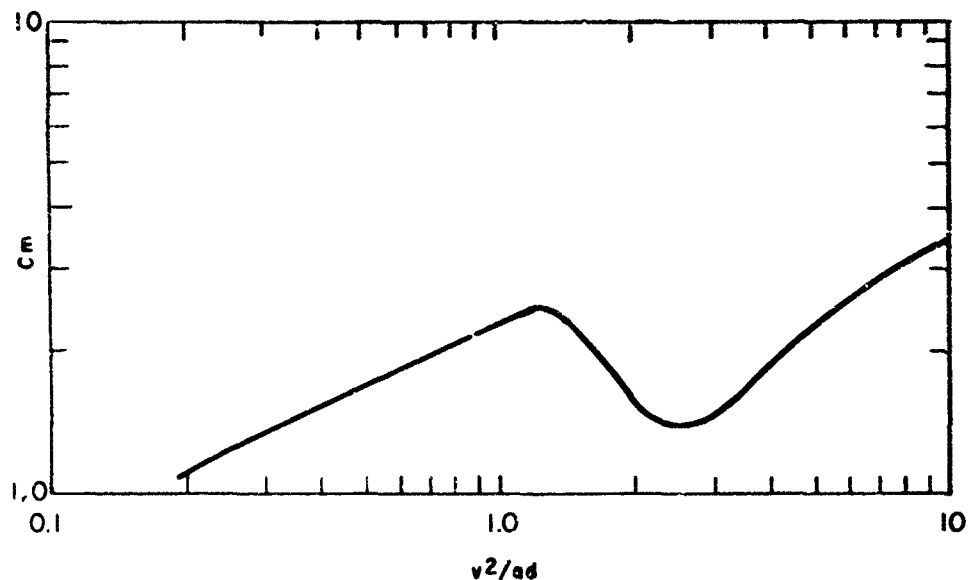


FIGURE 12 - Hydrodynamic Inertia Coefficient Versus Acceleration
Modules for 2 Long Thin Plate in Oscillatory Flow

Stanton and Marshall reported shedding of vortex rings from a disk at uniform velocity ($N_{Re} \approx 200$) with a periodicity corresponding to 8 diameters of travel. Using Hoerner's²⁷ empirical function for Strouhal number at Reynolds numbers above 10^3 ,

$$S_t = 0.21/C_D^{3/4}, \quad (22)$$

the Strouhal number for the circular disk is 0.192, and the distance for vortex shedding is 5.2 diameters. Vortices shed from the disk do not alternate as in the plate; therefore, one vortex would be shed every 5.2 diameters, or when $v^2/ad = y/d = 2.6$, for the oscillating disk.

It was noted in the oscillation tests that when the amplitude of disk motion was in the proximity of 3 diameters ($2y = 6d$), the disk became unstable and tended to skew to one side. This was attributed to vortex shedding during the motion cycle. The effect was clearly detrimental to the accuracy and credibility of the data beyond the critical amplitude, and the experiment was limited to lower amplitudes. It is important that utilization of the data of the present investigation be accompanied by the caveat against extrapolation.

Inversen and Balent, reporting on linear motion of disks, show scattered data above $v^2/ad = 5$, although the data below $v^2/ad = 5$ are well correlated. The discrepancy is attributed to side-wall interference and increasing inaccuracy in this range, but vortex shedding would appear to be a highly probable source of the scatter.

When the hydrodynamic inertia and drag effects are combined into a single drag force, the vortex anomaly, which occurs in the former but not in the latter, has an effect of far lesser magnitude, as Iversen and Balent's and Keulegan and Carpenter's data illustrate. Only the cylinder data of Keulegan and Carpenter are indicative of the vortex anomaly in the total resistance coefficient.

Description of an Oscillation Cycle

The oscillatory motion of a disk in a fluid is not a simple phenomenon, and it is instructive to follow the disk through the motion cycle, noting the various fluid-body interactions.

When the disk is approaching the centerline of motion, the velocity is nearing zero. The drag force, therefore, is increasing to its peak value as inertial resistance decreases. The moving disk has been accumulating and continues to accumulate a vortex ring that forms like a doughnut in the wake, enlarging and elongating along the direction of motion as the disk travels through the fluid. The energy associated with the acceleration of the vortex and the surrounding fluid, which is not entrained by the disk, but nevertheless, is set into motion by it, are, probably, the principal sources of hydrodynamic mass. Because the acceleration at this point is approaching zero, so too is the inertial effect of the hydrodynamic mass. At the instant when the harmonic velocity is maximum and harmonic acceleration is zero, the resistance force on the disk is entirely drag, as in the case of the constant velocity linear motion, and the hydrodynamic mass, although present, is undetectable.

During that portion of the motion cycle in which the velocity increases from zero to its maximum, the Reynolds number describing the motion increases from zero to some maximum value indicative of both laminar and turbulent conditions being experienced. However, as this motion cycle is just one in a long series of oscillations, the fluid has been disturbed by previous cycles, increasing the turbulent content of the motion.

As the disk passes the centerline of motion, the velocity begins to decrease and acceleration effects become more important. During this quarter cycle, drag decreases to zero and the hydrodynamic inertia increases toward a maximum. Reynolds number decreases again, and the comments made above apply. The vortex continues to grow. The condition for vortex shedding has not been attained as yet, since a distance of travel (or circumference of v^2/a) equivalent to six or eight disk diameters is required before sufficient vortex mass and elongation for shedding has been achieved. If the disk were to exceed the vortex shedding condition, the process of that shedding would cause an instability (presuming the disk is not rigidly maintained in orientation) to send the disk askew and cause considerable deviation from sinusoidal motion.

When the disk attains the endpoint of the motion cycle, velocity is zero and the disk is instantaneously motionless. The vortex in the disk's wake, however, is still in motion. It may be presumed that during the previous quarter-cycle, this vortex has been pushing somewhat on the disk, as the fluid entrained in the wake would lag the disk in decreasing its velocity, but at the point of zero velocity of the disk, the vortex impinges upon the disk, flowing over and around it. As the disk begins to reverse direction of travel, it must overcome the inertia of the vortex formed in its previous half-cycle and initiate the formation of a new vortex on the other side, in its wake as it travels again toward the centerline of motion, to repeat the events of the preceding half-cycle. It is the flow-reversal with the momentary vortex-body opposition which most distinguishes the oscillatory case from the linear one. The relative importance of this end-point-of-motion effect to the cyclical hydrodynamic inertia of the oscillating body is not clear, and a detailed analysis of the forces on the disk would be required to ascertain this.

CYLINDERS AND TANDEM DISKS

The emphasis of the present investigation was upon the determination of the hydrodynamic effects of harmonically accelerated disks; however, cylinders and disks in tandem were also considered, employing the same procedures heretofore applied to disks.

Cylinders

Although numerous investigations of a cylinder in motion transverse to its axis have been made, the cylinder in axial motion has been neglected. Two and one-half-inch diameter cylinders with length-to-diameter ratios (l/d) of 2, 1, and 0.025 (disks) were oscillated and values of hydrodynamic mass and drag determined.

The hydrodynamic inertia coefficient based upon the cylinder volume,

$$C_I = m_h / \rho (\pi/4) d^2 l, \quad (23)$$

was found to vary with the correlation modulus v^2/ad and l/d , as shown in figure 13. The results of Sarpkaya³ with parallelepipeds in small amplitude oscillation and Patton²² with parallelepipeds in large amplitude oscillation are shown for comparison. These data show the same trend of increased hydrodynamic mass with increased motion amplitude as the cylinder data ($y/d = v^2/ad$). The drag coefficient was unchanged between $l/d = 1$ and $l/d = 2$, as shown in figure 14 for several values of v^2/ad . The drag coefficient for cylinders in constant velocity axial flow from Hoerner²⁷ is also shown. The drag coefficient for unsteady flow approaches the steady flow value as v^2/ad increases, as in the case of the disk.

A total resistance coefficient C_T for cylinders was determined from equation (7), using C_I and C_D from figures 13 and 14, and is shown in figure 15. Decrease of C_T with both v^2/ad and l/d occurred.

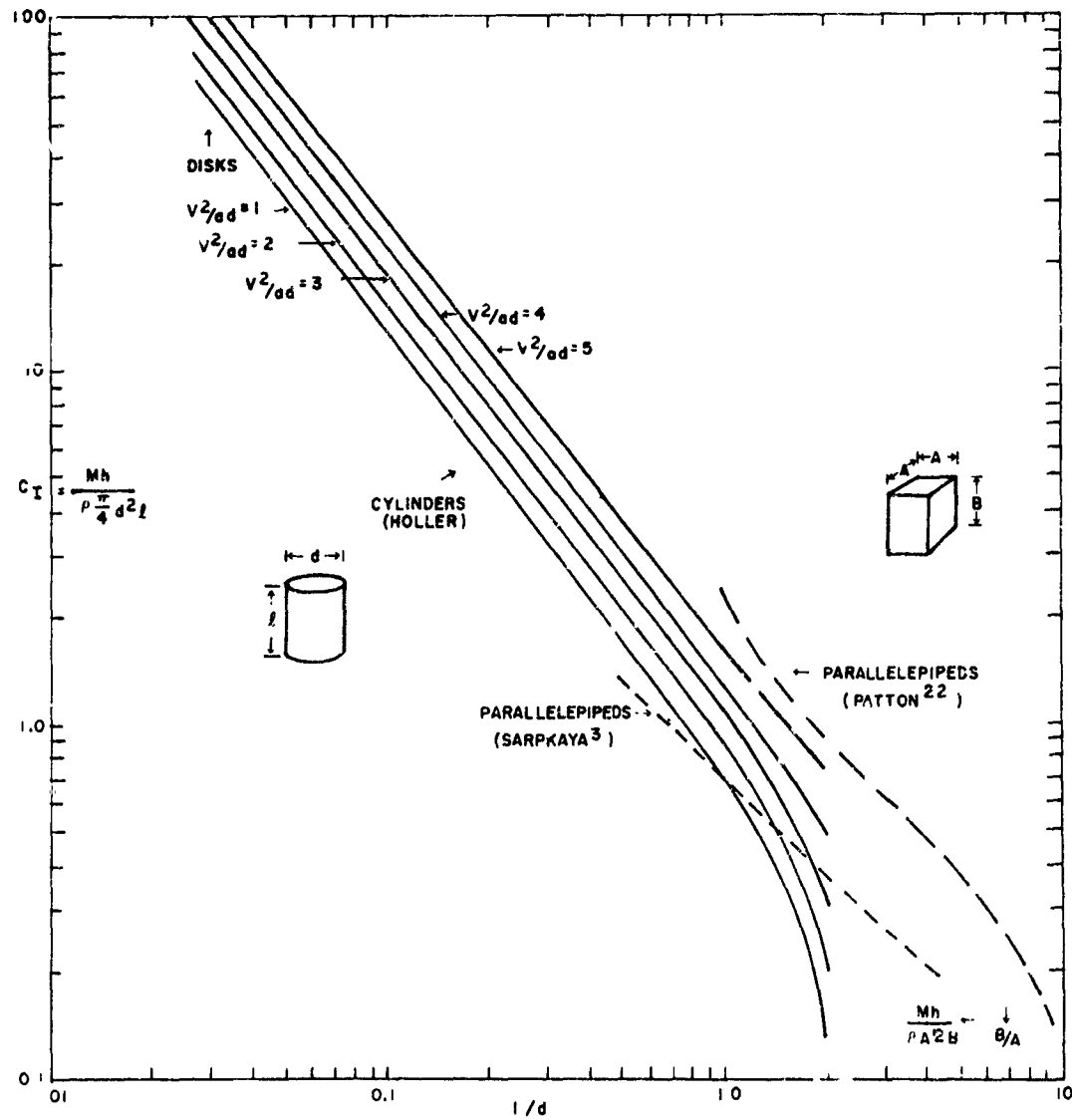


FIGURE 13 - Hydrodynamic Inertia Coefficient Versus Length-to-Diameter Ratio for Oscillating Cylinders

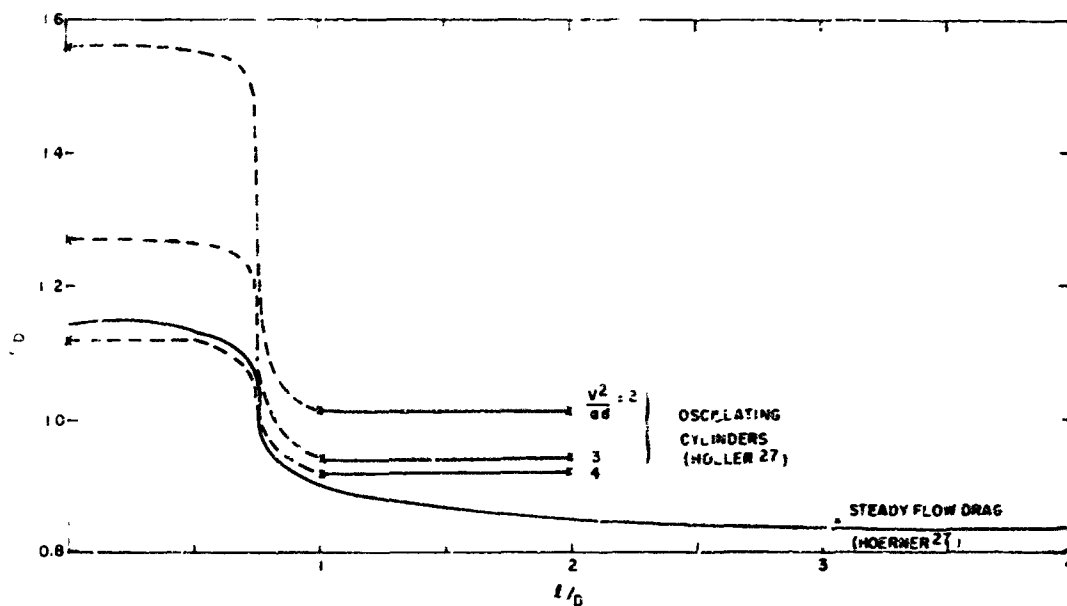


FIGURE 14 - Drag Coefficient Versus Length-to-Diameter Ratio for Oscillating Cylinders

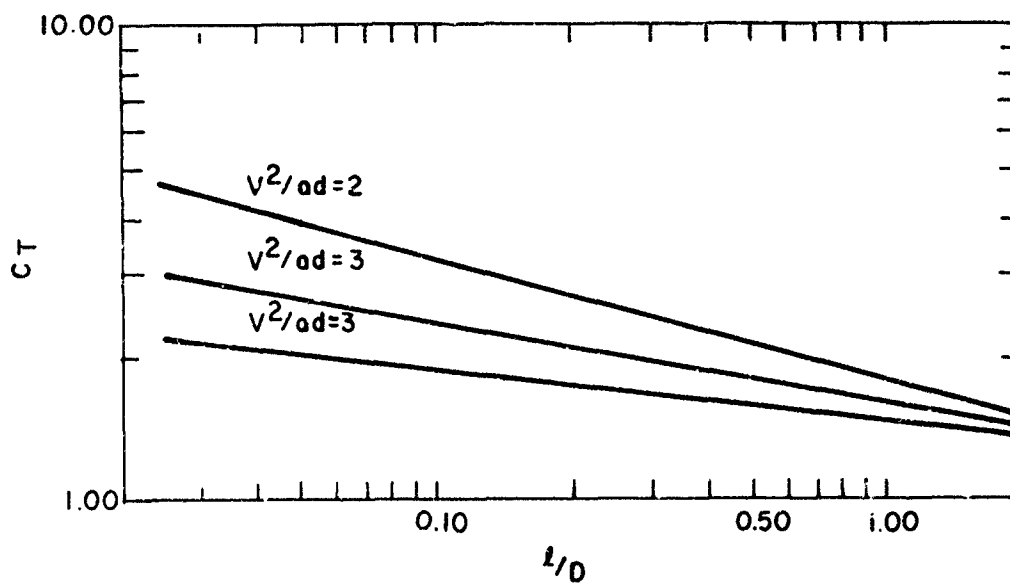


FIGURE 15 - Total Resistance Coefficient Versus Length-to-Diameter Ratio for Oscillating Cylinders

Tandem Disks

Two disks of equal diameters separated by a distance s were used to determine the hydrodynamic effects on oscillated tandem disks. The disks used were 4 and 6 inches in diameter and they were separated by a 1-inch diameter cylindrical rod.

The values of C_I obtained were based upon a characteristic volume of d^3 , as in the case of the single disk [equation (10)]. The hydrodynamic inertia coefficient is shown in figure 16 for various values of separation-to-diameter ratio (s/d) and v^2/ad . When s/d is very small, the data of the single disk apply. As separation increases slightly, the two disks maintain a semblance of the single disk, as the distance between the disks is too small, in relation to the disk size, to allow much flow in this gap. At somewhat more separation, a decrease in C_I occurs as destructive interference of the vortex trying to develop behind the forward disk with the rear disk takes place. This interference is evident for the range $0.1 < s/d < 0.5$, reaching a peak between 0.25 and 0.35, with some dependence upon v^2/ad . Beyond $s/d = 0.5$, the tandem disks begin to exceed the hydrodynamic mass of a single disk until at some large value of s/d (by extrapolation $s/d > 2$), the tandem disks perform as two separate disks.

Drag coefficient and total resistance coefficient for tandem disks are shown in figures 17 and 18, respectively. The characteristics of these two figures are much the same as in figure 16. It is noteworthy that Hoerner²⁷ describes the drag of tandem disks in steady flow by summation of a constant C_D associated with the forward disk and a C_D associated with the rear disk which is negative in the range $0 < s/d < 2.3$ and positive thereafter. The drag coefficient approaches that of two separate disks beyond $s/d = 7$. The negative drag on the rear disk is explained by the suction effect on it caused by the reduced dynamic pressure within the wake of the forward disk. As v^2/ad increases in figure 17, thus beginning to approach the case of steady flow, the value of s/d where C_D begins to exceed the drag coefficient of a single disk increases. The inset in figure 18, from Willmarth, et al.,²⁸ indicate a change in vortex interaction between tandem disks at $s/d = 0.35$, which approximates the condition noted in the present investigation.

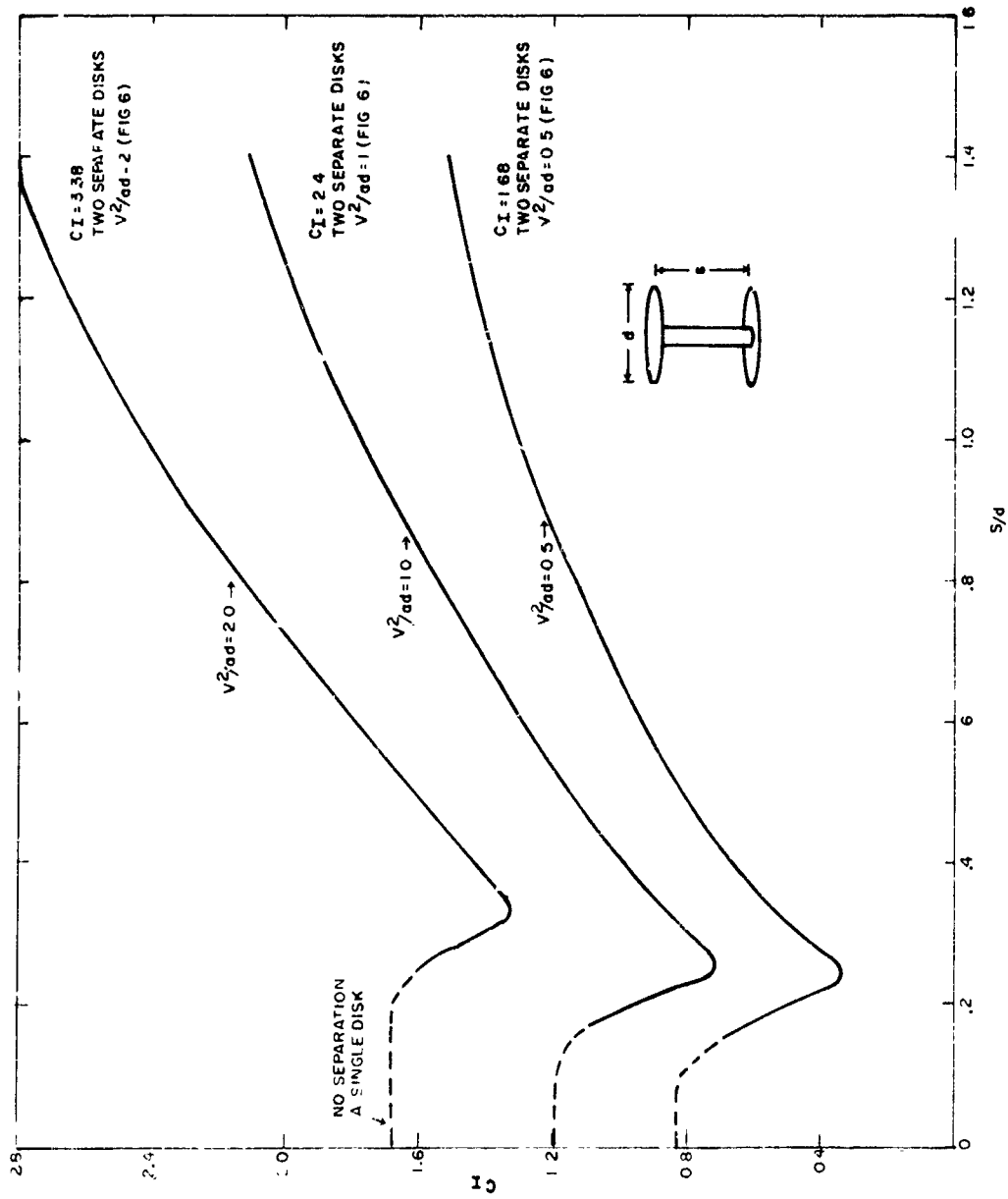


FIGURE 16 - Hydrodynamic Inertia Coefficient Versus Separation-to-Diameter Ratio for Oscillating Tandem Disks

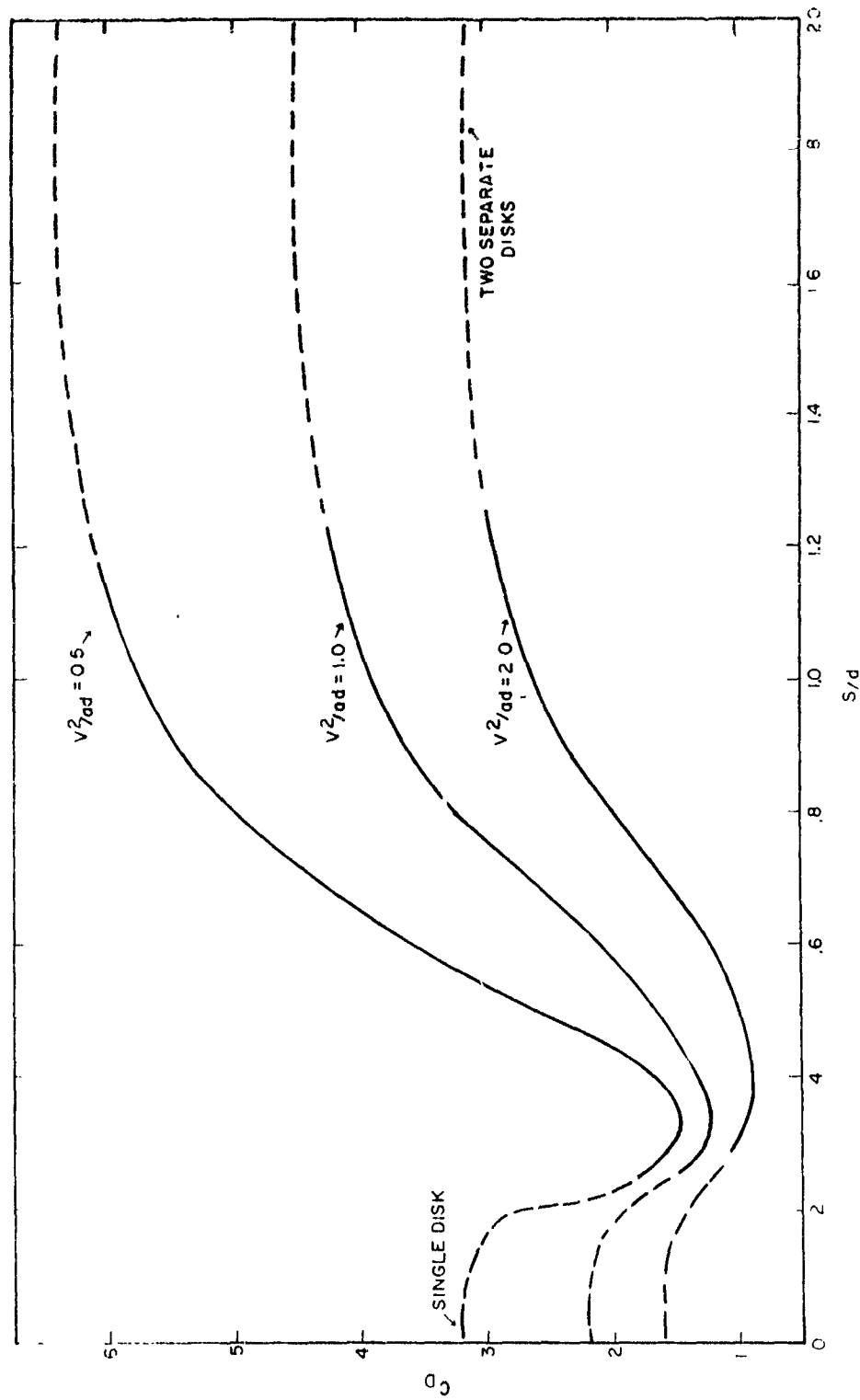


FIGURE 17 - Drag Coefficient Versus Separation-to-Diameter Ratio for Oscillating Tandem Disks

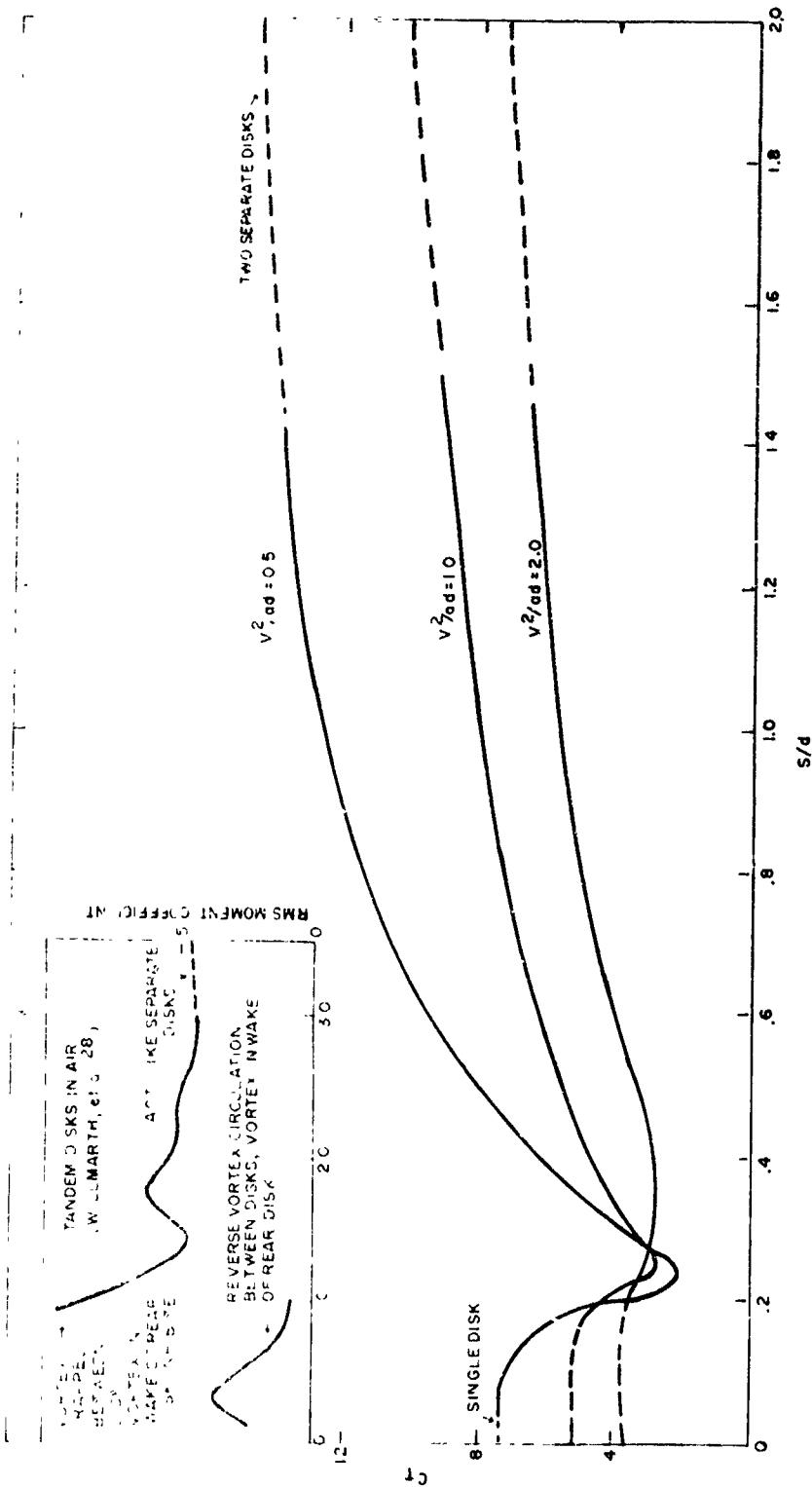


FIGURE 18 - Total Resistance Coefficient Versus Separation-to-Diameter Ratio for Oscillating Tandem Disks

R E F E R E N C E S

1. Sarpkaya, T.; Added Mass of Lenses and Parallel Plates, Proc. ASCE, J. Eng Mech Div, June 1960
2. Dale, J. R., and Holler, R. A.; Noise from Pressure Gradient Hydrophones Measured In Situ (U), U. S. Navy Journal of Underwater Acoustics, Vol 20, No. 2, April 1970 (CONFIDENTIAL)
3. Holler, R. A.; Mechanical Noise Evaluation of AN/SSQ-53 Sonobuoy Experimental Modifications in the Ocean Environment (U), Naval Air Development Center Report No. NADC-AE-7015, September 1970 (CONFIDENTIAL) AD512342L
4. Torobin, L. B., and Gauvin, W. H.; Fundamental Aspects of Solids-Gas Flow, Part III; Canadian J. Chemical Engineering, Vol 38, 1959
5. Stelson, T. E.; Accelerations of Bodies in Fluids - A Study in Virtual Mass; Ph.D. Thesis, Dept Civil Eng, Carnegie Institute of Technology, 1952
6. Milne-Thomson, L. M.; Theoretical Hydrodynamics: The MacMillan Company; New York, 1950
7. Kanwal, R. P.; Drag on an Axially Symmetric Body Vibrating Slowly Along its Axis in a Viscous Fluid; J. Fluid Mech, Vol 19, 1964
8. Carstens, M. R.; Accelerated Motion of a Spherical Particle; Trans Am. Geophys Union, Vol 33, No. 5, 1952
9. Kinsler, L. E., and Frey, A. R.; Fundamentals of Acoustics; John Wiley & Sons, Inc; New York, c. 1950
10. Stanton, T. E., and Marshall, D.; Eddy Systems Behind Discs; Aeronautical Research Committee (G.B.), Reports and Memoranda No. 1358, 1932
11. Simmons, N. S., and Dewey, L. F. G.; Wind Tunnel Experiments with Circular Discs; Aeronautical Research Committee (G.B.), Reports and Memoranda No. 1334, 1930
12. Willmarth, W. W., Hawk, N. E., and Harvey, R. L.; Steady and Unsteady Motions and Wakes of Freely Falling Disks; Physics of Fluids, Vol 7, No. 2, 1964
13. Bramig, R.; Experimental Determination of the Hydrodynamic Increase in Mass in Oscillating Bodies; David Taylor Model Basin (NSRDC) Translation 118, 1943

14. Iversen, H. W., and Balent, R.; A Correlating Modulus for Fluid Resistance in Accelerated Motion; J. Applied Physics, Vol 22, No. 3, 1951
15. Lunau, J.; Sur l'effet d'inertie des sillages de corps se deplacant dans un fluide d'un mouvement uniformement accelere; Compt ren Acad des Sci Paris, 1948
16. Keim, S. R.; Fluid Resistance to Cylinders in Accelerated Motion; Proc ASCE, J. of Hydraul Div, Paper 1113, 1956
17. Bugliarello, G.; La resistenze la moto accelerato di sfere in acqua; La Ricerca Scientifica, Vol 26, 1950
18. Lunnon, R. G.; Fluid Resistance to Moving Spheres; Proc Royal Soc London, Vol A118, 1928
19. Keulegan, G. H., and Carpenter, H. L.; Forces on Cylinders and Plates in an Oscillating Fluid; J. Research of National Bureau of Standards, Vol 60, No. 5, 1958
20. McNown, J. S., and Keulegan, G. H.; Vortex Formation and Resistance in Periodic Motion; Proc ASCE, J. Eng Mech Div, 1959
21. Crooke, R. C.; Re-analysis of Existing Wave Force Data on Model Piles; Beach Erosion Board, T.M. 71, 1955
22. Patton, K. T.; An Experimental Determination of Hydrodynamic Masses and Mechanical Impedances; M. S. Thesis, Dept Mech Eng, University of Rhode Island, 1965
23. Wiegel, R. L.; Oceanographical Engineering; Prentice-Hall, Inc; Englewood Cliffs, N. J., 1964
24. Murtha, J. P.; Virtual Mass of Partially Submerged Bodies; M. S. Thesis, Dept Civil Eng, Carnegie Inst Technology, 1954
25. Waugh, J. G., and Ellis, A. T.; Fluid - Free-Surface Proximity Effect on a Sphere Vertically Accelerated from Rest; J. Hydronautics, Vol 3, N. 4, 1969
26. Lohmert, R.; Akustische Messungen an Wirbelstrassen hinter Kreiszyylinder and ebener Platte; Physik Zeitschr, Vol 38, 1937
27. Hoerner, S. F.; Fluid-Dynamic Drag; Pub by author, 1958
28. Willmarth, W. W., Hawk, N. E., Galloway, A. J., and Roos, F. W.; Aerodynamics of Oscillating Disks and A Right-Circular Cylinder; J. Fluid Mech, Vol 27, pt 1, 1967

A P P E N D I X A

DETERMINATION OF THE HYDRODYNAMIC MASS AND
DAMPING CONSTANT OF OSCILLATING BODIES

The motion of the oscillating body submerged in a fluid is assumed to be described by the linear single-degree-of-freedom equation for a spring-mass system,

$$m\ddot{y} + c\dot{y} + ky = F \quad (A-1)$$

The undamped natural frequency of the system is

$$\omega_n^* = \sqrt{k/m_p} \quad (A-2)$$

where m_p is the physical mass and k the spring constant. In the fluid, the "undamped" natural frequency is

$$\omega_n = \sqrt{k/m} = \sqrt{k/(m_p + m_h)} \quad (A-3)$$

where m_h is the hydrodynamic mass and m is the virtual mass, $m = m_p + m_h$. The damped natural frequency in the fluid is

$$\omega_{nd} = \sqrt{k/m - (c/2m)^2} = \sqrt{\omega_n^2 - (c/2m)^2} \quad (A-4)$$

where c is the damping constant in the fluid (internal spring damping is negligible). The critical damping constant in the fluid is

$$c_c = 2 m \omega_n = 2 \sqrt{k(m_p + m_h)} \quad (A-5)$$

Combining equation (A-4) and equation (A-5)

$$(c/c_c)^2 = 1 - (\omega_{nd}/\omega_n)^2 \quad (A-6)$$

The magnification at a frequency ω is written

$$M = y/y_0 = \left\{ [1 - (\omega/\omega_n)^2]^2 + [2(\omega/\omega_n)(c/c_c)]^2 \right\}^{-1/2} \quad (A-7)$$

or

$$M = y/y_0 = k [(k - m\omega^2)^2 + \omega^2 c^2]^{-1/2} \quad (A-8)$$

At $\omega = \omega_n$,

$$M_n = c_c/2c \quad (A-9)$$

and at $\omega = \omega_{nd}$,

$$M_{nd} = \left\{ [1 - (\omega_{nd}/\omega_n)^2]^2 + 4(\omega_{nd}/\omega_n)^2 (c/c_c)^2 \right\}^{-1/2} \quad (A-10)$$

and substituting equation (A-6)

$$M_{nd} = \left\{ (c/c_c)^4 + 4(c/c_c)^2 [1 - (c/c_c)^2] \right\}^{-1/2} \quad (A-11)$$

Solving for $(c/c_c)^2$,

$$(c/c_c)^2 = (4 \pm \sqrt{16 - 12M_{nd}^2})/6 \quad (A-12)$$

and using equation (A-9)

$$M_n^2 = 6/(16 \pm \sqrt{16 - 12M_{nd}^2}) \quad (A-13)$$

Since M_{nd} and M_n must converge as damping approaches zero, i.e., M_n increases as M_{nd} increases, the sign in equation (A-13) is negative (-).
Writing

$$Q = \sqrt{16 - 12M_{nd}^2} \quad (A-14)$$

$$(c/c_c)^2 = (4 - Q)/6 \quad (A-15)$$

Combining equation (A-2) and equation (A-3)

$$(\omega_n^*/\omega_n)^2 = m/m_p = 1 + (m_h/m_p) \quad (A-16)$$

Using equation (A-4)

$$(\omega_n^*/\omega_{nd})^2 = (1 + m_h/m_p)/[1 - (c/c_c)^2] \quad (A-17)$$

$$m_h = m_p \left\{ (\omega_n/\omega_{nd})^2 [1 - (c/c_c)^2] - 1 \right\} \quad (A-18)$$

Substituting equation (A-15),

$$m_h = m_p [(2 + Q)/6] [(\omega_n^*/\omega_{nd})^2 - 1] \quad (A-19)$$

and

$$c = (m_p \omega_n^{*2} / \omega_{nd}) \sqrt{(4 - Q)(2 + Q)/9} \quad (A-20)$$

where Q is given by equation (A-14).

APPENDIX B

APPLICATION OF THE DATA TO SONOBUOY SUSPENSIONS

The sonobuoy suspension system may be considered as a spring-mass system governed by the linear single-degree-of-freedom equation. As might be expected, however, application of the results for the hydrodynamic effects of oscillating disks to this equation are not simple, and several alternative approaches are feasible.

Assumption A - The physical parameters of the spring-mass system (k , m_p), the operational frequency (ω), the input amplitude (y_0), fluid density (ρ), and disk diameter (d) are known. The amplitude of motion (y) is unknown.

1. Alternative One - Iterative Approach. The magnification equation can be written

$$y = y_0 k [(k - m\omega^2)^2 + \omega^2 c^2]^{-1/2} \quad (B-1)$$

a. Set $m = m_p + m_h$ and use figures 6 and 9 where

$$cv = \rho C_D A v^2 / 2 \quad (B-2)$$

or the equation

$$C_I = 1.2 (y/d)^{1/2} \quad (B-3)$$

$$C_D = 2.2 (y/d)^{-1/2} \quad (B-4)$$

or

b. Set $m = m_p$ and use figure 10 or the equation

$$C_T = 5.2 (y/d)^{-1/2} \quad (B-5)$$

where

$$cv = \rho C_T A v^2 / 2 \quad (B-6)$$

Estimate a value for y and determine the corresponding values of m_h and/or c to substitute in equation (B-1). If the resulting y does not equal the original estimate, alter the estimate and repeat the procedure until the y obtained from the equation and the estimate are equal.

2. Alternative Two - Reduced variables approach. Combining equations (B-2), (B-3), and (B-4) yields

$$1.44c = m_p \omega \quad (B-7)$$

and equation (B-1) can be written relating y to either m_p or to c . Iteration can be used to determine y , or the equation (B-3) or equations (B-2) and (B-4) can be used to write a single equation in y . This equation is

$$\omega^4 (\alpha^2 - \beta) y^3 + 2\alpha\omega^2 (m_p \omega^2 - k) y^{5/2} + (k - m_p \omega^2)^2 y^2 = y_0^2 k^2 \quad (B-8)$$

where

$$\alpha = 1.2 \rho d^{5/2} \quad (B-9)$$

and

$$\beta = \omega^2 d^5 / 1.44 \quad (B-10)$$

This equation may be used with an iteration approach somewhat simpler than the previous alternative, or solved numerically.

3. Alternative Three - Total resistance approach using equation (B-5) and (B-6)

$$c^2 = \gamma^2 \gamma \omega^2 \quad (B-11)$$

where

$$\gamma = 2.04 \rho d^{5/2} \quad (B-12)$$

Substituting in equation (B-1) yields

$$y^3 + [(k - m_p \omega^2) / \gamma \omega^2]^2 y^2 - (y_0 k / \gamma \omega^2)^2 = 0 \quad (B-13)$$

a cubic equation in the form

$$y^3 + A^2 y^2 - B^2 = 0 \quad (B-14)$$

Again, iteration may be applied or numerical solution computed. Knowing A and B , the equation may be graphed

$$F(y) = y^3 + A^2 y^2 - B^2 \quad (B-15)$$

Graphing $F(y)$ against y , the function has a maximum at $y = -2A^2/3$ where $F(y) = [(4A^6/27) - B^2]$ and a minimum at $y = 0$ where $F(y) = -B^2$. Therefore, $F(y)$ crosses the y -axis ($F(y) = 0$) in three places, with two negative and one positive value of y , if $A^6/B^2 > 27/4$; $F(y)$ is tangent to the y -axis, with two equal negative values and one positive value of y , if $A^6/B^2 = 27/4$; and $F(y)$ crosses the axis only once, with two imaginary values and one positive real value of y , if $A^6/B^2 < 27/4$. In each case, there exists one real positive value of y which satisfies equation (B-14). The use of this graphical method is illustrated in figure B-1 where $A^2 = 2$ and $B^2 = 3$ have been chosen arbitrarily. Intersection of $F(y)$ and the y -axis yields the value of y which satisfies the equation.

The equation (B-14) can also be used to generate a graph as shown in figure B-2 where constant y curves are plotted for values of A^2 and B^2 . For the above example of $A^2 = 2$ and $B^2 = 3$, the value of y obtained is shown to agree with the value obtained by graphing $F(y)$.

Assumption B - The physical parameters of the spring-mass system (k , m_p), the operation frequency (ω), the input amplitude (y_0), fluid density (ρ), and the desired amplitude of motion (y) are known. The disk diameter (d) is unknown.

Several methods, similar to the above solutions for y may be used, determining the value of d from the values of m_h and c . Equation (B-13) can be used directly since y is known to give

$$\gamma^2 = (y_0 k / \omega^2)^2 (1/y^3) - (k - m_p \omega^2)^2 (1/y) \quad (B-16)$$

and using equation (B-12)

$$d^5 = (y_0 k / \rho \omega^2)^2 (1/4.16 y^3) - [(k - m_p \omega^2) / \rho \omega^2]^2 (1/4.16 y) \quad (B-17)$$

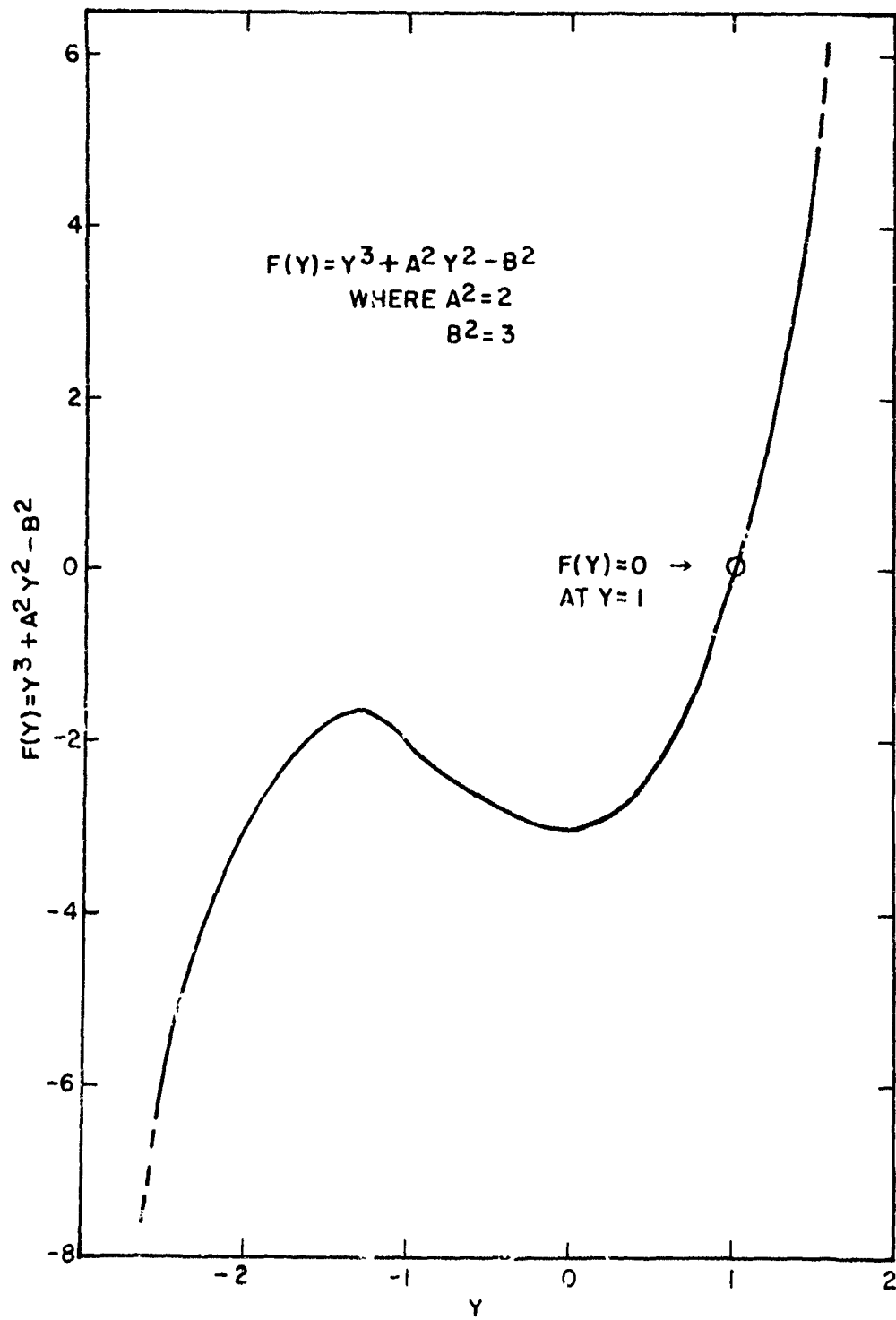


FIGURE B-1 - Graphical Solution of the Total Resistance Equation

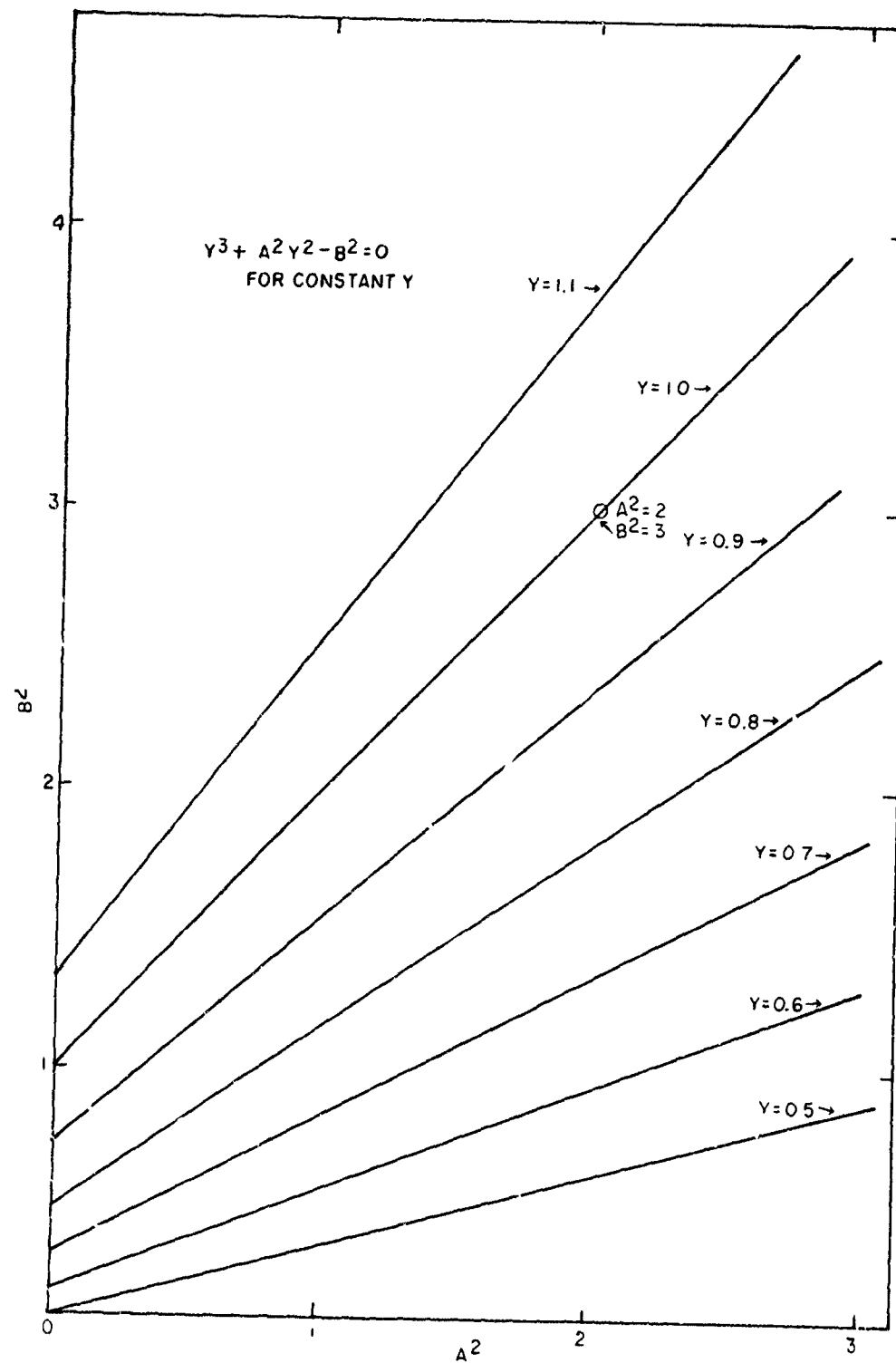


FIGURE B-2 - Constant Amplitude Plot of the Total Resistance Equation